

# A rolling tachyon field for both dark energy and dark halos of galaxies

M.B.Causse\*

March 27, 2019

Groupe d'Astroparticules de Montpellier, IN2P3/CNRS, Université Montpellier II Place E.Bataillon, CC085, 34095 Montpellier Cedex 5 France

## Abstract

Distance measurements to type Ia supernovae (SNe Ia) indicate that the universe is accelerating and it is spatially flat. Otherwise, the rotation curves for galaxies or galaxy clusters reveal the existence of a dark matter component. Then, approximately 0.35 of the total energy density of the universe consists of dark matter, and 0.65 of the energy density corresponds to dark energy. These two dark components of the universe have different properties such that: dark matter clusters gravitationally at galactic scales while dark energy, dominating at large scale, does not cluster gravitationally. It seems difficult to find a candidate which explains the observations at both large and small scales. In this paper we take into account a scalar field, more precisely a rolling tachyon arising from string theory, which seems to be capable to explain the observations at different scales. We examine this scalar field behavior at galactic scales and we fit the rotational curve data of spiral galaxies. Our results are comparable with the curves obtained on one hand from a complex scalar field, which only plays the role of the dark matter at galactic scales, and on the other hand from the MOND model.

## 1 Introduction

The observational data of our Universe, at different scales, reveal that our Universe is dominated by a Dark density component. Indeed, the measurement of type Ia supernova light curves by two groups, the Supernova Cosmology Project [1] and the High-z Supernova Team [2], leads to the conclusion: the Universe is speeding up, not slowing down. Otherwise, an independent line of evidence for the accelerating Universe comes from measurements of the composition of the universe. The Cosmic Microwave Background (CMB) anisotropy measurements indicate that the Universe is flat [3], so the total density is:  $\Omega_c = 1$ . Moreover, in a flat universe the matter density ( $\Omega_M$ ) and energy density ( $\Omega_{DE}$ ) must sum to the critical density:  $\Omega_M + \Omega_{DE} = \Omega_c$ , where matter contribution is:  $\Omega_M = 0.33 \pm 0.04$  [4], leaving two thirds of the dark energy ( $\Omega_{DE} \simeq 0.65$ ). In order to have escaped detection, this dark energy must be smoothly distributed. In order not to interfere with the formation of cosmic structure, the energy density in this component must change more slowly than matter, so that it was subdominant in the past. Theorists have been very busy suggesting all kinds of interesting possibilities for the dark energy. Dark energy is a negative pressure component with an equation of state as  $p = \omega \rho$  with  $\omega$  negative, not necessary constant. One of the possible explanations is the existence of a non-zero vacuum energy, i.e a “cosmological constant” where  $\omega = -1$ . For candidates like homogeneous tachyon field([5]) or scalar field (quintessence) [6],  $\omega$  is time dependent and can vary between  $-1$  and  $+0$ .

---

\*causse@gamum2.in2p3.fr

mean star velocity did not drop off with radius from the galactic center as rapidly as the fall-off in luminous mass in the galaxy dictated according to Newtonian gravity. The stars far from the center were rotating too fast to be balanced by the gravitational force from the luminous mass contained within that radius. This led to the proposition that most of the mass in a galaxy was low luminosity mass of some kind, and this invisible mass was called Dark Matter (DM)[7]. The amount of dark matter present in the universe has been estimated using various techniques, including observing the velocities of galaxies in clusters [8] and calculating the gravitational mass of galactic clusters by their gravitational lensing effects on surrounding spacetime. Then, the matter density is the sum of baryonic density  $\Omega_B = 0.05$  and dark matter density  $\Omega_{DM} = 0.25$ . So, the rotation curves (RCs) of spiral galaxies [9] are the most natural way to model dark matter. Contrary to the dark energy component, the dark matter component, with an equation of state:  $p = 0$ , clusters gravitationally at galactic scales. Particle physics provides an attractive solution to the non baryonic dark matter problem. Long-lived or stable particles with very weak interactions can remain from the earliest moments of the universe in sufficient numbers to account for a significant fraction of critical density.

Due to the supersymmetry (SUSY) breaking mechanisms, the supersymmetric theories offer the most promising explanations concerning the dark energy and cold dark matter components of the universe. However, the nature of the supersymmetric candidates depend on the scale. Indeed, in the Minimal Supersymmetric Standard Model (MSSM), where soft SUSY breaking terms are present, the lightest neutralino is a good candidate for the cold dark matter [10] but not for the dark energy. The dark energy is due to a scalar field, the quintessence field. And, the determination of the shape of the quintessence potential depends on the SUSY breaking<sup>1</sup> mechanism. Then, the quintessence field is not a good candidate to explain the observations at both small and large scales (although, some scalar fields can play the dark matter role [17] only). Recent work on tachyon field (arising from string theory) in cosmology ([5],[12],[13] and [14]) tends to show that a tachyon field can behave like dark energy with negative pressure at large scale and can cluster gravitationally on small scales. So, if the fine-tuning problem can be explained, the tachyon field is a viable candidate to explain the observations at both small and large scales. In this context, we consider a tachyon field model, given by T. Padmanabhan and T.R.Choudhury in reference [14], thanks to which it is possible to obtain different equations of state at different scales. At large scales, the authors have shown that this model reproduces the correct behavior. Our study concerns the behavior of this field on small scales and more precisely its contribution to the dark matter component of the universe. By simplicity we retain only the Newtonian solution and fit the rotation curve data of spiral galaxies.

This paper is organized as follows. In section 2, we quickly review the tachyon scalar field model and develop the Newtonian solution of the tachyonic Lagrangian considered. In section 3, we present the plots of the spiral galaxies rotation curves obtained with this type of tachyonic dark matter. Finally, in section 4 we conclude.

## 2 The tachyon scalar field model

In the string theoretical context, a tachyonic Lagrangian arises naturally. This is a generalization of the Lagrangian for a relativistic particle and it takes the following form:

$$L_{tach} = -V(\phi)\sqrt{1 - \partial^i\phi\partial_i\phi} \quad (1)$$

where  $\phi$  is the tachyon field and  $V(\phi)$  the potential.

This theory admits solutions where the two following conditions:  $V \rightarrow 0$ ,  $\partial_i\phi\partial^i\phi \rightarrow 1$  can be met simultaneously. Such solutions have finite momentum density and energy density. Then, the solutions can depend on both space and time and the momentum density can be an arbitrary function of the spatial coordinate. Thus, this context seems to be adapted at the same time to large and small scales in cosmology.

---

<sup>1</sup>However, SUSY breaking scale, at least of the order of 1 Tev, is the crucial point to achieve in explicit string models. Indeed, such a breaking must arise from nonperturbative effects which are often difficult to control [11].

The model considered is given by T. Padmanabhan and T.R.Choudhury in reference [14]. We quickly review the principal ingredients. For more details, the reader is referred to [14]. This model takes into account the gravitational interaction modified by a scalar field and a scalar potential. The effective low energy action is:

$$S = \int d^4x \sqrt{-g} \left( \frac{R}{16\pi G} - V(\phi) \sqrt{1 - \partial^i \phi \partial_i \phi} \right) \quad (2)$$

where  $R$  is the curvature scalar,  $G$  the gravitation constant ( $\bar{h} = c = 1$ ) and  $g$  the determinant of the metric. Moreover, the field  $\phi$  is regarded as a scalar field for simplicity. The Einstein equations are

$$R_k^i - \frac{1}{2} \delta_k^i R = 8\pi G T_k^i \quad (3)$$

and the stress tensor for the scalar field can be written in a perfect fluid form

$$T_k^i = (\rho + p) u^i u_k - p \delta_k^i \quad \text{with } u_k = \frac{\partial_k \phi}{\sqrt{\partial^i \phi \partial_i \phi}} \quad \text{and } u_k u^k = 1 \quad (4)$$

The density and the pressure are respectively:

$$\rho = \frac{V(\phi)}{\sqrt{1 - \partial^i \phi \partial_i \phi}}; \quad p = -V(\phi) \sqrt{1 - \partial^i \phi \partial_i \phi} \quad (5)$$

This stress tensor can be put in the form according to:

$$\rho = \rho_{DE} + \rho_{DM} \quad (6)$$

$$p = p_{DE} + p_{DM}$$

with the two different equations of state:

$$\rho_{DM} = \frac{V(\phi) \partial^i \phi \partial_i \phi}{\sqrt{1 - \partial^i \phi \partial_i \phi}} \quad \text{and } p_{DM} = 0 \quad (7)$$

$$\rho_{DE} = V(\phi) \sqrt{1 - \partial^i \phi \partial_i \phi} \quad \text{and } p_{DE} = -\rho_{DE}$$

Thus, we notice that the stress tensor can be broken up into the sum of two components, one having the behavior of dark energy and the other one the dark matter behavior. However, the scalar field  $\phi$  must have a particular configuration to account for the equations of state on different scales. Then, the effective field<sup>2</sup> that we chose has the following form:

$$\bar{\phi}(t, r) = A(r)t + f(r) \exp(-2t) \quad (8)$$

where the functions,  $A(r)$  and  $f(r)$ , determine the evolution of the field on the various scales. The time dependence is related to the potential

$$\bar{V}_r(\bar{\phi}(t, r)) = V_0 \exp\left(-\frac{\bar{\phi}(t, r)}{\phi_0}\right) \quad (9)$$

At large scales, the rate of the expansion of the universe is determined by  $A(r)$ . Indeed, when  $r$  increases the fluctuations decrease, so  $\phi(r)$  will be a decreasing function of  $r$  thus  $A(r)$  will have a value less than unity. Taking  $\phi(r) = A(r) = \text{constant}$  and  $V = V_0 / \exp(A(r)t)$  one can find consistent set of solutions for an  $\Omega = 1$  Friedmann-Robertson-Walker model with a power expansion  $a(t) \propto t^n$  and  $A(r) = \sqrt{\frac{2}{3n}}$ .

---

<sup>2</sup>The effective field is the average of a field  $\phi(t, x)$  over a length scale  $r$  ([12], [13] and [16])

( $t \rightarrow \infty$ ) and  $\rho_{DE} \approx 0$  what implies that:  $V \rightarrow 0$  and  $\partial_i \phi \partial^i \phi \rightarrow 1$ , thus  $A(r) \rightarrow 1$ . In this context we have

$$\rho_{DM} \approx \frac{V_0}{\sqrt{4f(r)}} \text{ for } \phi_0 \sim 1/2 \text{ and } \rho_{DE} \approx 0 \quad (10)$$

the pressureless component dominates at galactic scales and the associated density is independent of time ([12], [13]). This resembles the non-interacting dark matter and the field  $\bar{\phi}(t, r)$  can play the role of dark matter.

We have just seen that this scalar field can give an account at the same time of dark energy and dark matter components of the universe. The next step is now to study the behavior of this field at galactic scales.

## 2.2 Newtonian solution

In this section, we consider the scalar field  $\phi$  as the dark matter of the universe at galactic scales. Under these conditions, the expression of the field takes the following form:

$$\bar{\phi}(t, r) = A(r)t + f(r) \exp(-2t) \text{ with } A(r) \rightarrow 1 \quad (11)$$

The analytical expression of  $f(r)$  is given by the solution of the differential equation for the scalar field. This equation is obtained from the Lagrangian (2), the Einstein equations (3) and (4) and the Klein Gordon equation for a massless field. Moreover, the spherically symmetric solutions are characterized by the Schwarzschild metric:

$$ds^2 = \exp(\nu(r))dt^2 - \exp(\lambda(r))dr^2 - r^2(d\theta^2 + \sin^2\theta d\varphi^2) \quad (12)$$

where  $\nu(r)$  and  $\lambda(r)$  are constant for the Newtonian solutions.

Then, the differential equation for the scalar field is given by

$$f''(r) + \frac{2}{r}f'(r) - 4f(r) = 0 \quad (13)$$

where  $' = \frac{d}{dr}$ . For simplicity, we take  $\exp(\lambda(r) - \nu(r)) = 1$  since  $\nu(r)$  and  $\lambda(r)$  are constant.

The Newtonian form of  $f(r)$  reads

$$f(r) = \frac{1}{r}(C_1 \sinh(2r) + C_2 \cosh(2r)) \quad (14)$$

where  $C_1$  and  $C_2$  are two constants, with  $C_2 = 0$ , so that the solution is not singular at the origin. Taking into account the equations (14) and (10) the density energy expression takes the following form:

$$\rho_{DM} = \frac{V_0}{\sqrt{4f(r)}} = \frac{V_0}{2\sqrt{C_1}} \sqrt{\frac{r}{\sinh(2r)}} \quad (15)$$

For small  $r$ , we have  $\rho \propto \frac{V_0}{2\sqrt{2C_1}}(1 - \frac{r^2}{3} + \frac{r^4}{10})$ , i.e. it is proportional to a constant  $C = \frac{V_0}{2\sqrt{2C_1}}$ . This constant resembles a core radius. Otherwise, the mass function is given by  $M(x) = \int_0^x \rho(r)r^2 dr$  then we obtain

$$M(x) = C \int_0^x \frac{r^{(5/2)}}{\sqrt{\sinh(2r)}} \quad (16)$$

Therefore, we shall model rotation curves of spiral galaxies. Observational data show that rotation curves are becoming flat in the surrounding region of galaxies where data are received from the 21cm wavelength of neutral hydrogen (HI). We introduce dark matter consisting of the massless scalar field which interacts with the luminous matter exclusively by the gravitational force. We apply only Newtonian solutions of our model.

the velocity  $v_\phi^2 \simeq \frac{C'}{x}$  then:

$$v_\phi^2 \simeq \frac{C}{x} \int_0^x \frac{r^{(5/2)}}{\sqrt{\sinh(2r)}} \quad (17)$$

The behavior of  $v_\phi$  is presented in figure 1, for  $C' = 90km/s$  (with  $C' = \sqrt{C}$ ). At low  $x$ , this curve presents a maximum and an asymptotic value for large  $x$ .

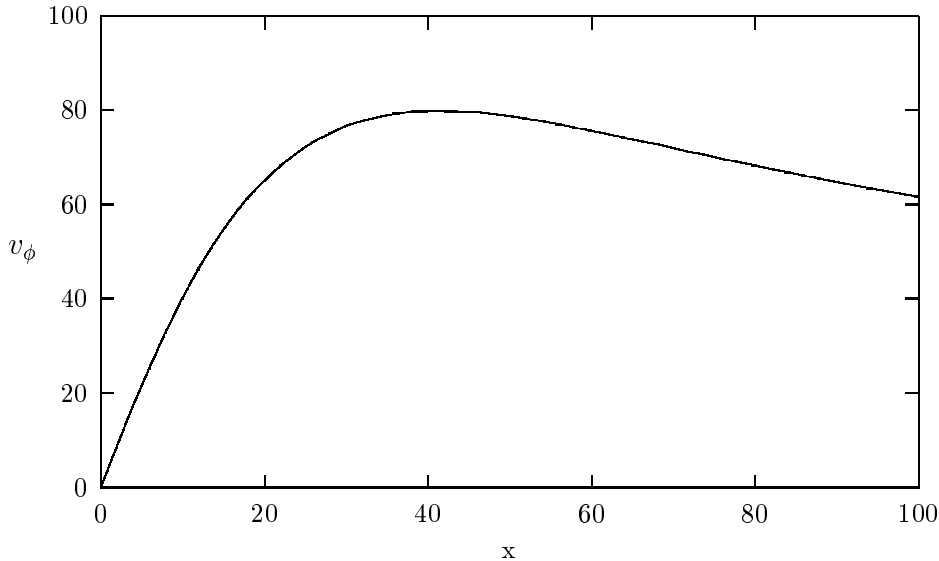


Figure1: A rotation curve  $v_\phi$  for a value of  $C' = 90km/s$  where the velocity is in  $km/s$  and  $x$  in  $kpc$ .

### 3 Rotation curves for spiral galaxies

To model rotational curves of spiral galaxies, we use the universal rotation curves of Persic, Salucci and Stel [9]<sup>3</sup> and some individual ones [15]. The total rotation curves result from a combination of several components, i.e. the stellar disk, the halo, the gas and the bulge of the galaxy

$$v_{total} = \sqrt{v_{disk}^2 + v_{halo}^2 + v_{gas}^2 + v_{bulge}^2} \quad (18)$$

The rotation curve for stellar disk follows from an exponential thin disk light distribution and the halo contribution is given by  $v_\phi$ .

#### 3.1 Universal rotation curves

The universal rotation curves [9] depend on two components: the stellar disk and our halo

$$v_{total} = \sqrt{v_{disk}^2 + v_{halo}^2} \quad (19)$$

The contribution from the stellar disk can be written as:

$$v_{disk}^2(x) = V^2(R_{opt})\beta \frac{1.97 x^{(1.22)}}{(x^2 + 0.78^2)^{1.43}} \quad (20)$$

---

<sup>3</sup>However, universal rotation curves, depending only on the luminosity, don't represent very well the data in some cases[18]

blue band is  $M_B = -20.5$  and  $M_B = -0.58 + 0.92M_I$  ( $M_I$  for the  $I$  band). The constants in the  $\beta$  function are arranged in order to obtain the best fit for our rotational curves. The equation (20) is valid within the range  $0.04 \simeq x \leq 2$ .

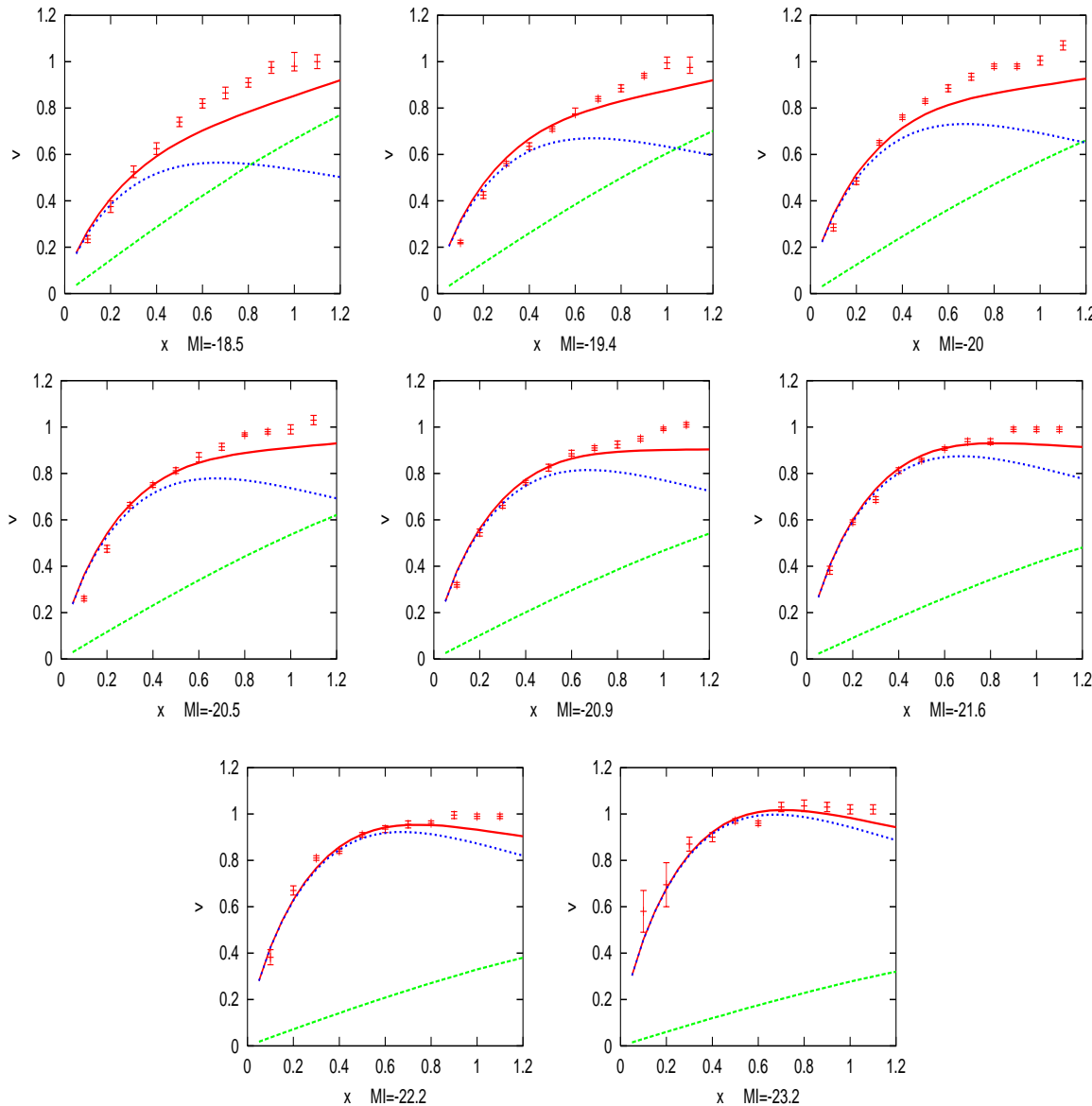


Figure2: Height universal rotation curves arranged by absolute magnitudes  $MI$ , the radial coordinate  $x$  in units of the optical radius  $x_{opt}$  and the velocity  $v$  in units of  $v(opt)$ . The halo curve is represented by a green line (or gray dotted line) for initial values  $C' = 1.5, 1.36, 1.29, 1.21, 1.05, 0.93, 0.74, 0.62$  corresponding to  $MI = -18.5$  for the first and  $MI = -23.2$  for the last value. The blue (black dotted) and red (continuous) lines are respectively the disc curve and the total rotation curve.

---

<sup>4</sup> $R_{opt}$  is the optical radius such as  $R_{opt} \equiv 3.2R_D$  where  $R_D$  is the disk exponential length-scale.

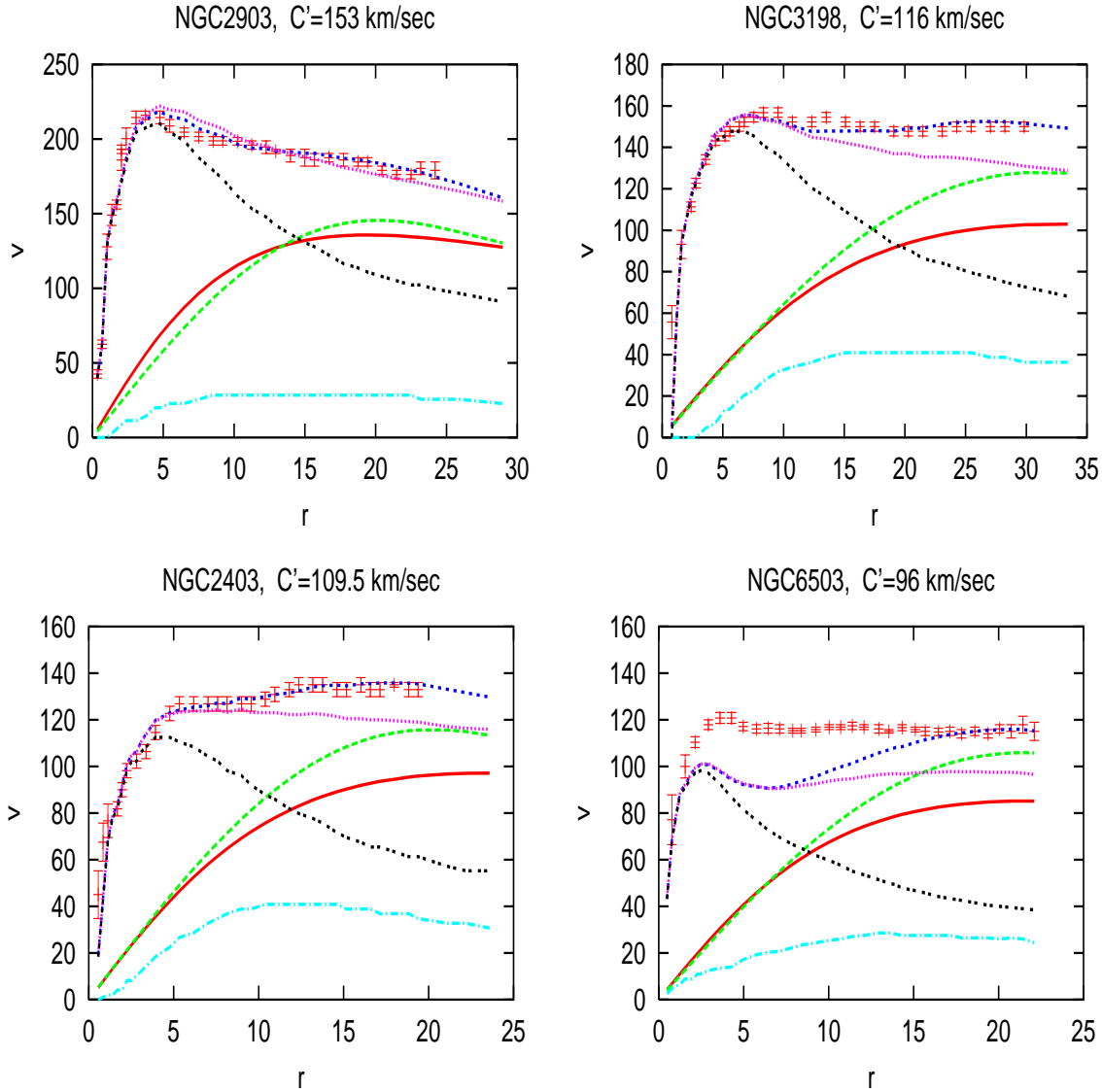


Figure3: Rotation curve fits for NGC6503, NGC2403, NGC3198 and NGC2903 with our halo (red or black continuous), stars (black dotted) and HI gas (light blue or gray dashed-dot). Our rotation curves are the pink (or gray dotted) curves. The curves associated to the scalar complex field are green (or gray long-dashed) for the velocity of the field and dark-blue (or dark-gray dotted) for the rotation curves. The velocity is measured in [km/s] and the radial coordinate  $r$  in [kpc]

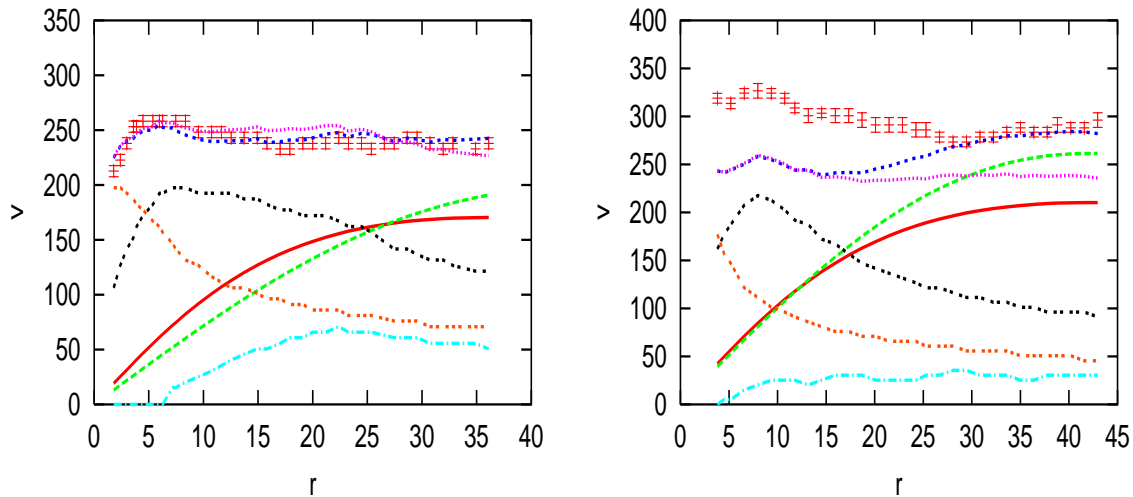


Figure4: Rotation curve fits for NGC7331 and NGC2841 with bulge. Our halo (red or black continuous), stars (black dotted), bulge (red or gray dotted) and HI gas (light blue or gray dashed-dot) are represented. Our rotation curves are the pink (or gray dotted) curves. The curves associated to the scalar complex field are green (or gray long-dashed) for the velocity of the field and dark-blue (or dark-gray dotted) for the rotation curves. The velocity  $v$  is measured in [km/s] and the radial coordinate  $r$  in [kpc]

Our halo contribution depends on the parameter  $C'$  only. At each absolute magnitude  $M_I$  corresponds one  $C'$  value.

The main results are shown in Fig.2. This figure shows eight observational rotation curves with different absolute magnitudes  $M_I$  as well as the fitted curves using equation (19). The individual contributions from disk and the scalar field are also shown. From the observational data, we see that low luminosity spiral galaxy has a rather increasing rotation curve and a high luminosity spiral galaxy a rather decreasing rotation curve. This means that a spiral galaxy with low luminosity is stronger dominated by a dark matter halo than a spiral one with high luminosity. Our model has the same behavior. Indeed, for low luminosity, the scalar field contribution is more significant than in the case of high luminosity. This fact is related to the parameter  $C'$  which only determines the halo far from the luminosity matter region. Unfortunately, for low luminosity corresponding to  $M_I = -18.5$  for the first and  $M_I = -20.9$  for the last one, we don't have a good agreement of the data. Our curves are below the data with an order of magnitude of 20% for the first and 15% for the other ones. For high luminosity we obtain a rather good agreement with the data.

### 3.2 Spiral galaxies rotation curves

In this subsection, we consider two type of individual spiral galaxies ([15] and [17]), some of them with bulge and the others one without. Four galaxies, where the stellar disk, gas and halo components contribute to the rotation curves, are shown in figure 3. In figure 4, we present two spiral galaxies in which a clear bulge can be read off the light curve. For each individual galaxies, in order to obtain the best fit for our rotational curves, the  $C'$  parameter is deduced from the observational data and the disk component so that:  $C' \simeq v_{disk}$  in the range where the observational rotation curve becomes flat. Moreover, for each spiral galaxy,  $v_\phi$  reaches its maximum at the radial coordinate  $r$  corresponding to the last observational point. The data for rotation curve fits are listed in Table (1).

Concerning the spiral galaxies without bulge, the rotation curves are presented in figure 3. Figure 3 shows the observational data, the individual contributions from luminous matter, the gas and our halo of four different spiral galaxies. The comparison with a scalar complex field, [17] ( $\Psi(r, t) = P(r) \exp(-i\omega t)$ ) which plays only the role of dark matter, is also shown. The maximum observed



		( $Mpc$ )	( $km/sec$ )	( $10 M_{\odot}$ )	( $kpc$ )	( $km/sec$ )
NGC2903	$Sc(s)I-II$	6.40	216	15.30	24.18	153
NGC3198	$Sc(rs)I-I$	9.36	157	9.00	29.92	116
NGC2403	$Sc(s)III$	3.25	136	7.90	19.49	109.5
NGC6503	$Sc(s)II.8$	5.94	121	4.80	22.22	96
NGC7331	$Sb(rs)I-I$	14.90	257	54.00	36.72	192
NGC2841	$Sb$	9.46	326	20.50	42.63	237

Table 1: Data for rotation curve fits

rotation velocity for the galaxy NGC6503 is  $v_{max} = 121km/sec$  and the order of  $\sim 216km/sec$  for the NGC2903. In these curves, we remark that the agreement between our model and the observational data, is sensitive to the maximum observed rotation velocity. Indeed, for the spiral galaxy NGC2903, we obtain a very good agreement of the data as for the scalar complex field. When the velocity decreases, i.e. for NGC2403 ( $v_{max} = 136km/sec$ ) and NGC3198 ( $v_{max} = 157km/sec$ ), our curves are below the data in the surrounding region, with an order of magnitude of 10% for the first one and 15% for NGC3198 whereas the complex field model describes the data perfectly. In the case of the Modified Newtonian Dynamics (MOND) model [19], the rotation curves agree well with the observed curve for NGC2403 and for NGC3198 the differences are in the opposite sense (about 15%). However, concerning the spiral galaxy NGC6503, our model as well as the complex scalar field don't reproduce the observational data.

The spiral galaxies, NGC7331 ( $v_{max} = 257km/sec$ ) and NGC2841 ( $v_{max} = 326km/sec$ ), with bulge are presented in figure 4. For NGC7331, our model (like the scalar complex field and the MOND model) reproduces the observational data perfectly. Unfortunately, we obtain very bad results for NGC2841 in the inner regions (about 30%), as in the case of the scalar complex field. However, in the outer regions the scalar complex field model gives good agreement with the data while our model is lower (about 20%). In the MOND [19] model, the predicted curve is significantly higher than observed in the inner regions (about 15%) and comparably lower in the outer regions.

Finally, we conclude that the considered tachyonic field (eq.11) [14] gives interesting results at galactic scales, for reasonable velocities. For extreme velocities such as:  $121km/s$  (NGC6503) and  $326km/s$  (NGC2841), our model as well as the complex scalar field (and MOND model) don't reproduce the observational data. In this context, such field seems to be a viable candidate to explain the observations at both small and large scales.

## 4 Conclusion

In this paper, we were interested in a tachyon field [14] (arising from string theory ref.[5],[12],[13]) which can behave like dark energy with negative pressure at large scales and can cluster gravitationally on small scales. Such tachyon field seems to be a viable candidate to explain the observations at both small and large scales. Here, we have studied the behavior of this tachyonic field at galactic scales and more precisely its contribution to the dark matter component of the universe. By simplicity, we have retained only the Newtonian solution of the Lagrangian considered. In this context, we have fitted the rotation curves of six spiral galaxies (two with bulge and four without bulge).

Our rotation curves show that this model gives interesting results. Indeed, for the galaxies NGC2903 and NGC7331 we obtain a good agreement with the data and reasonable results for the other ones. our results are comparable with the curves obtained on the one hand from a complex scalar field, which only plays the role of the dark matter at the galactic scales, and on the other hand from the MOND model. To conclude, we think that such tachyonic field is a viable candidate to explain the observations at both small and large scales.

**ACKNOWLEDGMENTS:** This work was partly supported by Euro-Gdr SUSY. I am grateful to K.Jedamzik and H.Reboul for several useful discussions. I am also thankful to P.Brax,

# References

- [1] M.Perlmutter et al, Phys.Rev.Lett.83, 670, 1999;  
Perlmutter et al, APJ.517,565, 1999.
- [2] Riess.A. et al,AJ,116,1009, 1998.
- [3] Sievers, J.L. et al, A.J.591:599-622,2003.
- [4] Turner, M.S. A.J.576:L101-L104, 2002.
- [5] H.K.Jassal astro-ph/0303406; J.S.Bagla,  
H.K.Jassal and T.Padmanabhan Phys.Rev.D67, 063504,(2003);  
A.Sen, JHEP 0204, 048 (2002) [hep-th/0203211, 0203265, 0212198].  
V.Gorini et al hep-th/0311111.
- [6] P.Brax, J.Martin and A.Riazuelo Phys.Rev.D62:103505,2000;  
B.Ratra and P.J.E.Peebles Phys.Rev.D37,3406, 1988.  
P.G.Ferreira and M.Joyce Phys.Rev.D58,023503, 1998;  
M.Sami, P.Chingamgam, T.Qureshi Phys.Rev.D66:043530, 2002 (hep-th/0205179)  
M.Fairbain, M.Tygart Phys.Lett.B546 (2002) 1-7.  
I.Zlatev, L.Wang and P.J.Steinhardt Phys.Rev.Lett.82, 896, 1999 and Phys.Rev.D59, 123504,  
1999.
- [7] F.Zwicky, Helv.Phys.Acta6, 110, 1933
- [8] S.Smith Astro.J.83, 23, 1936
- [9] M.Persic, P.Salucci and F.Stel Mon.Not.Astron.Soc.281:27, 1996.  
A.Borriello and P.Salucci astro-ph/0001082 and astro-ph/0011079.  
P.Salucci and A.Burkert A.J.537:L9-L12, 2000.  
H.Hoeskstra, T.S. van Albada and R.Sancisi astro-ph/0010569.
- [10] A.Falvard et al. astro-ph/0210184.
- [11] I.Antoniadis, E.Dudas and A.Sagnotti Phys.Lett.B464:38-45, 1999
- [12] A.Sen JHEP0204:048, 2002 and Mod.Phys.Lett.A17:1797-1804, 2002.  
M.C.Bento et al. Phys.Rev.D67:063511, 2003.  
T.Pamanabhan and T.Roy Choudhury Mon.Not.Roy.Astron.Soc.344:823-834, 2003.
- [13] G.Shui and I.Wasserman Phys.Lett.B541:6-15, 2002.  
A.Frolov, L.Kofman & A.Starobinsky Phys.Lett.B545:8-16, 2002.  
G.W.Gibbons Phys.Lett.B537:1-4, 2002.
- [14] T.Padmanabhan and T.Roy Choudhury Phys.Rev.D66:081301, 2002.
- [15] K.G.Begeman, A.H.Broeils and R.H.Sanders Mon.Not. R. astr. Soc. (1991) 249, 523-537.  
P.D.Mannheim and J.Kmetko astro-ph/9602094.  
T.Matos AIP Conf.Proc.490:382-387, 1999.  
T.Matos and F.S.Guzman astro-ph/9810028.  
F.S.Guzman, T.Matos and B.H.Villegas Rev.Mex.Astron.Astrophys.37:63-72,2001.  
M.Marcelin et al.A&A 1983:128, 140.
- [16] T.Padmanabhan Phys.Rev.D66:021301,2002 (hep-th/0204150)
- [17] F.E.Shunck astro-ph/9802258

Sofue Y. et al., 1999, *ApJ*, 823, 136.

Y.Sofue and V.Rubin astro-ph/0010594.

Verheijen M.A.W., 1997, Ph.D. thesis Rijksuniversiteit Groningen.

[19] R.Bottema et al.: *A&A*,393: 453-460, 2002.